OXFORD

Genome analysis

Deconvoluting multiple infections in *Plasmodium falciparum* from high throughput sequencing data

Sha Joe Zhu [1,*]**, Jacob Almagro-Garcia** [1] **and Gil McVean** [1,2,*]

[1] Wellcome Trust Centre for Human Genetics, University of Oxford, Oxford OX3 7BN, UK
[2] Big Data Institute, Li Ka Shing Centre for Health Information and Discovery, University of Oxford, Oxford OX3 7BN, UK

[*] To whom correspondence should be addressed.

Abstract

Motivation: The presence of multiple infecting strains of the malarial parasite *Plasmodium falciparum* affects key phenotypic traits, including drug resistance and risk of severe disease. Advances in protocols and sequencing technology have made it possible to obtain high-coverage genome-wide sequencing data from blood samples and blood spots taken in the field. However, analysing and interpreting such data is challenging because of the high rate of multiple infections present.

Results: We have developed a statistical method and implementation for deconvoluting multiple genome sequences present in an individual with mixed infections. The software package *DEploid* uses haplotype structure within a reference panel of clonal isolates as a prior for haplotypes present in a given sample. It esimates the number of strains, their relative proportions and the haplotypes present in an sample, allowing researchers to study multiple infection in malaria with an unprecedented level of detail.

Availability and implementation: The open source implementation *DEploid* is freely available at https://github.com/mcveanlab/dEploid under the conditions of the GPLv3 license. An R version is available at https://github.com/mcveanlab/DEploid-r.

Contact: joe.zhu@well.ox.ac.uk or mcvean@well.ox.ac.uk

Supplementary information: Supplementary data are available at *Bioinformatics* online.

1 Introduction

Malaria remains one of the top global health problems. The majority of malaria related deaths are caused by the *Plasmodium falciparum* parasite (WHO, 2016), transmitted by mosquitoes of the genus *Anopheles*. Patients are often infected with more than one distinct parasite strain (termed mixed infection, multiple infection, or complexity of infection), due to bites from multiple mosquitoes, mosquitoes carrying multiple genetic types or a combination of both. Mixed infections can lead to competition among co-existing strains and may influence disease development (de Roode et al., 2005), transmission rates (Arnot, 1998) and the spread of drug resistance (de Roode et al., 2004). In addition, within-host evolution can lead to the presence of more than one genetically and phenotypically distinct strains (Bell et al., 2006).

The presence of multiple strains of *P. falciparum* makes fine scale analysis of genetic variation challenging, since genetic differences between strains of this haploid organism will appear as heterozygous loci. Such mixed calls confound methods that exploit haplotype data to detect, among other phenomena, the occurrence of natural selection or recent demographic events (Harris and Nielsen, 2013; Lawson et al., 2012; Mathieson and McVean, 2014; Sabetil et al., 2002). In light of these difficulties, researchers usually focus on clonal infections or resort to heuristic methods for resolving heterozygous genotypes. The former approach discards valuable information regarding genetic diversity and relatedness, whereas the latter tends to create chimeric haplotypes that are not suitable for analysis, unless mixed calls are very sparse.

In comparison to the problem of phasing haplotypes within diploid organisms, deconvoluting the strains of a multiple infection differs because of uncertainty in the number of strains present and their relative proportions. Consequently, existing tools for phasing diploid organisms, such as Beagle (Browning and Browning, 2007), IMPUTE2 (Howie et al., 2009) and SHAPEIT (Delaneau et al., 2012; O'Connell et al., 2016), are not appropriate. Galinsky et al. (2015) and O'Brien et al. (2015) have attempted to address the multiple infection problem by inferring the number and proportions of strains from allele frequencies within samples.

However, since they do not infer haplotypes, these approaches have limited applicability.

As part of the Pf3k project (Pf3k, 2016), an effort to map the genetic diversity of *P. falciparum* at global scale, we have developed algorithms and a software package implementation `DEploid`, for deconvoluting multiple infections. The program estimates the number of different genetic types present in the isolate, the proportion or abundance of each strain and their sequences (i.e. haplotypes). To our knowledge, `DEploid` is the first package able to deconvolute strain haplotypes and provides a unique opportunity for researchers to study the epidemiology of *P. falciparum*.

2 Methods

2.1 Notations

We first introduce our notation (see Table 1). Our data, D, are the allele read counts of sample j at a given site i, denoted as $r_{j,i}$ and $a_{j,i}$ for reference (REF) and alternative (ALT) alleles respectively. These are assigned values of 0 and 1 reseptively. Here we consider only biallelic loci, though future extension to include multi-allelic sites is simple. The empirical allele frequencies within a sample (WSAF) $p_{j,i}$ and at population level (PLAF) f_i are calculated by $\frac{a_{j,i}}{a_{j,i}+r_{j,i}}$ and $\frac{\sum_j a_{j,i}}{\sum_j a_{j,i}+\sum_j r_{j,i}}$ respectively. Since all data in this section refers to the same sample, we drop the subscript j from now on.

i	Marker index
j	Sample index
r	Read count for reference allele
a	Read count for alternative allele
f	Population level allele frequency (PLAF)
n	Number of strains within sample
l	Sequence length
$\mathbf{w}$	Proportions of strains
$\mathbf{x}$	Log titre of strains
$\mathbf{h}_i$	Allelic states of n parasite strains at site i
$h_{k,i}$	Allelic state of parasite strain k at site i
p	Observed within sample allele frequency (WSAF)
q	Unadjusted expected WSAF
π	Adjusted expected WSAF
Ξ	Reference panel
e	Probability of read error

Table 1. Table summarising the notation used in this article.

2.2 Model

We descibe the mixed infection problem by considering the number of strains, n, the relative abundance of each strain, $\mathbf{w}$, and their allelic states, $\mathbf{h}$. Similar to O'Brien et al. (2015), we use a Bayesian approach and define the posterior probabilities of n, $\mathbf{w}$ and $\mathbf{h}$ given a reference panel, Ξ, and the read error rate, e, as:

$$P(n, \mathbf{w}, \mathbf{h}, |\Xi, e, D) \propto L(n, \mathbf{w}, \mathbf{h}, |\Xi, e, D) \times P(n, \mathbf{w}, \mathbf{h}). \quad (1)$$

We assume a prior in which the haplotypes of the n strains are independent of each other and dependent only on the reference panel. Therefore, the joint prior can be written as:

$$P(n, \mathbf{w}, \mathbf{h}) = P(n) \times P(\mathbf{w}|n) \times \prod_{k=1}^{n} P(h_k|\Xi). \quad (2)$$

The following sections describe details of the model and the approach to inference.

2.2.1 Likelihood function

Let $\mathbf{w} = [w_1, \ldots, w_n]$ and $\mathbf{h}_i = [h_{1,i}, \ldots, h_{n,i}]$ denote the proportions and allelic state of the n parasite strains at site i. We use O'Brien et al. (2015)'s expression for the expected WSAF at site i, q_i, as:

$$q_i = (\mathbf{w} \cdot \mathbf{h}_i) = \sum_{k=1}^{n} w_k \cdot h_{k,i}. \quad (3)$$

The data, which can be summarised by the reference and alternative allele read counts at each site, is modelled through a beta-binomial distribution given the WSAF. We model the data at distinct segregating sites as independent. Thus the likelihood function in Eqn. (1) is only dependent on the haplotypes present and their frequencies through their contribution to q_i; i.e. $L(n, \mathbf{w}, \mathbf{h}, |\Xi, e, D) = \prod_{i=1}^{l} L(q_i|\Xi, e, D)$.

To incorporate sequencing error, we modify the WSAF such that the expected allele frequency of 'REF' read as 'ALT' is $(1 - q_i)e$, and the expected allele frequency of 'ALT' read as 'REF' is $q_i e$. Thus, the adjusted WSAF becomes:

$$\pi_i = q_i + (1 - q_i)e - q_i e = q_i + (1 - 2q_i)e. \quad (4)$$

We model over-dispersion in read counts relative to the Binomial using a Beta-binomial distribution. Specifically, the read counts of 'ALT' are identically and independently distributed (i.i.d.) Bernoulli random variables with probability of success v_i; i.e. $a_i \sim Binom(a_i + r_i, v_i)$, and $v_i \sim Beta(\alpha, \beta)$, where $E(v_i) = \alpha/(\alpha+\beta) = \pi_i$. This is achieved by setting $\alpha = c \cdot \pi_i$ and $\beta = c \cdot (1 - \pi_i)$, such that the variance of the WSAF is inversley proportion to c. Combined, we have:

$$L(q_i|e, D) \propto \frac{\Gamma(a_i + c \cdot \pi_i)\Gamma(r_i + c \cdot (1 - \pi_i))}{\Gamma(c \cdot \pi_i)\Gamma(c \cdot (1 - \pi_i))}. \quad (5)$$

2.2.2 Prior distributions

Rather than model the number of strains, n, directly, we take the approach of fixing n to be at the upper end of what can realistically be inferred (typically 5), using a skewed prior for proportions (such that typically only $1 - 2$ strains might be at appreciable frequency) and then discarding strains inferred to have a proportion less than some critical amount (e.g. 1 percent).

To achieve this, we model the proportions of the n strains through a log titre, x_k, drawn from a $N(\eta, \sigma^2)$ prior. The proportion of strain k, w_k, is given by

$$w_k = \frac{\exp(x_k)}{\sum_{j=1}^{n} \exp(x_j)}, \quad (6)$$

and the prior density is given by the distribution function for the value of $\mathbf{x}$.

Haplotypes, $\mathbf{h}$, are modelled as being generated independently from the reference panel by the Li and Stephens (2003) process, though with a rate of mis-copying that is independent of the panel size. That is, under the prior, a path through the reference panel is sampled as a Markov process where recombination enables switching between members of the reference panel and mis-copying allows the allelic state of the haplotype within the sample to differ from the allelic state of the reference panel haplotype being copied at the site. The transition probability of switching from copying reference haplotype a to reference haplotype b is $(1 - \exp(-\psi_i))/|\Xi|$, where ψ_i is the genetic distance (in Morgans) between sites i and $i+1$ and

$|\Xi|$ is the size of the reference panel. Note that unlike the original model the recombination or switching rate is not dependent on sample size.

For emission probabilities, let ξ_k denote the state of the sequence in the reference panel Ξ that h_k is copying from at given site and μ denote the probability of miss-copying:

$$\begin{cases} P(\xi_k = h_k) = 1 - \mu, \\ P(\xi_k \neq h_k) = \mu. \end{cases}$$

As above, this is a simple reparamterisation of the original model, but where the emission probabilities are not dependent on the sample size.

2.3 Inference

To perform inference about the haplotypes present and their proportions we use Markov chain Monte Carlo (MCMC). We use a Metropolis-Hastings algorithm to sample proportions ($\mathbf{w}$) given $\mathbf{h}$; and use a Gibbs sampler to update $\mathbf{h}$ for a given $\mathbf{w}$, with two types of update: a single haplotype and a pair of haplotypes.

2.3.1 Metropolis-Hastings update for proportions
We update $\mathbf{w}|n$, through the underlying log titres, $\mathbf{x}|n$. Specifically, we choose i uniformly from n and propose new x_i's from $x_i' = x_i + \delta x$, where $\delta x \sim N(0, \sigma^2/s)$, and s is a scaling factor. The new proposed proportion is therefore $\frac{\exp(x_k')}{\sum_{k=1}^n \exp(x_k')}$. Since the proposal distribution is symmetrical, the Hastings ratio is 1. A new update is accepted with probability

$$\min\left(1, \frac{P(\mathbf{w}'|n)}{P(\mathbf{w}|n)} \frac{L(\mathbf{w}', \mathbf{h}, \Xi, e|D)}{L(\mathbf{w}, \mathbf{h}, \Xi, e|D)}\right).$$

2.3.2 Gibbs update for single haplotype
We choose haplotype strain s uniformly at random from n strains to update. At each site, given the current proportions, we can calculate the likelihood of the 0 and 1 states. To achieve this, we first remove it from the current WSAF, i.e. subtract $w_s \cdot h_s$ from Eqn. (3), which gives

$$q_{i,-s} = \sum_{k \neq s} w_k \cdot h_k = \text{Eqn. (3)} - w_s \cdot h_s. \tag{7}$$

Therefore, updating the allelic state of strain s to 0 and 1, the expected WSAF becomes

$$q_{i,h_s=0} = \text{Eqn. (7)} \tag{8}$$

$$q_{i,h_s=1} = \text{Eqn. (7)} + w_s \times 1. \tag{9}$$

We substitute Equations (8) and (9) into Equation (5) after adjustment for read error.

Given the structure of the hidden Markov model and the above likelihoods, the forward algorithm can be used to sample a path through the reference panel, and subsequent mis-copying, efficiently from the marginal posterior distribution. In effect, the reference panel is used as a prior on haplotypes present in the sample (with recombination creating a mosaic of the different haplotypes) and the mis-copying process allows for recent mutation, recurrent mutation, gene conversion and some types of technical error. Figure 1) illustrates the approach.

2.3.3 Gibbs update for a pair of haplotypes
In order to improve mixing, we also perform Gibbs-sampling updates for pairs of haplotypes (given current proportions). The algorithm proceeds as for the single-haplotype update, though with a larger state space. First, we sample a pair of haplotypes, s_1 and s_2, uniformly. As in Equation (7), we first remove their states from the WSAF:
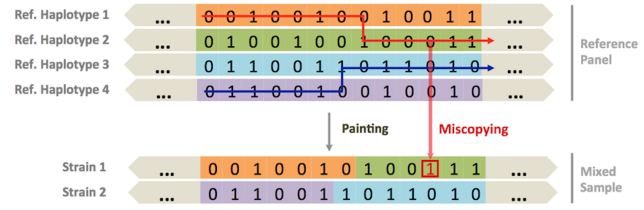

Fig. 1. The Li and Stephens (2003) algorithm as applied to the problem of multiple strain inference. Strain 1 haplotype is made up from reference haplotype segments of 1 and 2; and strain 2 haplotype is made up from reference haplotype segments of 3 and 4. With mis-copying, we allow strain states differ from the path: At the third last position of strain 1, the path is copied from reference haplotype 2, with the state of 0.

$$q_{i,-s_1,-s_2} = \sum_{k \neq s_1, s_2} w_k \cdot h_k$$
$$= \text{Eqn. (3)} - w_{s_1} \cdot h_{s_1} - w_{s_2} \cdot h_{s_2}. \tag{10}$$

Considering all four possible combination of genotypes, we can then write down the expected WSAF:

$$q_{i,h_{s_1}=0,h_{s_2}=0} = \text{Eqn. (10)} \tag{11}$$

$$q_{i,h_{s_1}=0,h_{s_2}=0} = \text{Eqn. (10)} + \cdot w_{s_1} \times 1 \tag{12}$$

$$q_{i,h_{s_1}=0,h_{s_2}=1} = \text{Eqn. (10)} + \cdot w_{s_2} \times 1 \tag{13}$$

$$q_{i,h_{s_1}=0,h_{s_2}=1} = \text{Eqn. (10)} + \cdot w_{s_1} \times 1 + w_{s_2} \times 1. \tag{14}$$

Substituting expressions. (11) to (14), into Equation (5), we then obtain their associated likelihoods.

As in the single-haplotype update, the hidden Markov model formulation enables us to sample a pair of paths through the reference panel (and the mis-copying process) efficiently from the marginal posterior distribution using the forward algorithm, that is given the other haplotypes and their inferred proportions. Equations describing the calculations are given in the Supplementary Material.

2.4 Implementation details

- **Number of strains**. As described above, we aim to infer more strains than are actually present, starting the MCMC chain with a fixed n, which has a default of 5. At the point of reporting, we discard strains with a proportion less than a fixed threshold, typically 0.01.
- **Parameters**. In practice, we set the parameters $c = 100$ (Equation (5)); $\eta = 0$, $\sigma^2 = 3$ and $s = 40$ (Sections 2.2.2 and 2.3.1). We set the read error rate as 0.01 and the rate of mis-copying as 0.01.
- **Recombination rate and scaling**. We assume a uniform recombination map, where the genetic distance between loci i and $i + 1$ is computed by $G_i = D_i/d_m$ where D_i denotes the physical distance between loci i and $i + 1$ in nucleotides and d_m denotes the average recombination rate in Morgans^{-1}. We use a recombination rate for *P. falciparum* of 15,000 base pairs per centiMorgan reported by Miles et al. (2016)). Suppose the genetic distance ψ_i is given by $\psi_i = 2N_e G_i$, with $N_e = 10$ being the effective population size. In reality, N_e is just a scaling parameter (not the effective population size). We then use the genetic distance ψ to compute the transition probability of switching from copying reference haplotype a to reference haplotype b (see Supplementary Materials for details).

- **Update without linkage disequilbrium**. For initialising the chain, or if the markers present are very widely spaced, linkage disequilibrium can be ignored, which is equivalent to setting the genetic distance between adjacent loci to be infitely high. Under these circumstances, the haplotype updates become much simpler and depend only on the population-level allele frequency (PLAF).
- **Reporting** We aim to provide users with a single point estimate of the haplotypes and their proportions, although the full chain is also available for analysis. To achieve this we report values at the last iteration - i.e. we report a single sample from the posterior. However, to measure robustness, we also typically repeat deconvolution with multiple random starting points and select the chain with the lowest average deviance (after removing the burn-in) to report. The deviance measures the difference in log likelihood between the fitted and saturated models, the latter being inferred by setting the WSAF to that observed. These parameters can be modified by users to achieve a preferred balance between computational speed and confidence. By default, we set the MCMC sampling rate as 5; burn the first 50% of the states; and keep 800 samples.
- **Reference panel construction**. To infer clonal samples for the reference panel we use the Pf3k (Pf3k, 2016) project data, running the algorithm without LD on all samples and identifying those with a dominant haplotype (proportion > 0.99) as clonal. These clonal samples are grouped by region of sampling to form location-specific reference panels.

3 Validation and Performance

As validation we used a set of *in vitro* mixtures created by Wendler (2015) to simulate mixed infections. DNA was extracted from four laboratory parasite lines: 3D7, Dd2, HB3 and 7G8, and mixed by different proportions (see Table 2; figures in brackets), and submitted to the MalariaGEN pipeline (MalariaGEN, 2008) for Illumina sequencing and genotyping (Manske et al., 2012).

This data set only contains two unmixed samples, which is insufficient for constructing a reference panel. Moreover, the *P. falciparum* genetic crosses project (Miles et al., 2016) found that due to sequencing error, mapping error and variation among variant calling methods, genotype calls vary at the same locus for the same strain of *P. falciparum*. To create a basline reference haplotype for each strain we therefore considered mutiple samples that contains the same parasite strains.

Inferring haplotypes for Dd2 strain. Since 3D7 is the reference strain, we assume that strain Dd2 is the only source of 'ALT' reads in samples PG0389-C to PG0394-C. Assuming markers are independent from each other, let y be the read count for 'ALT' allele and x be the total read count weighted by the Dd2 mixing proportion (see Table 2 in brackets), we use a regression model ($y = \beta_0 + \beta_1 x$) to infer the Dd2 genotype: 1 if β_1 is significant with p-values below 0.001; 0 otherwise.

Inferring haplotypes for HB3 and 7G8. Similarly, for samples PG0398-C to PG0415-C, we let variables x_1, x_2 be the coverages weighted by the mixing proportions of HB3 and 7G8 respectively; we use a regression model ($y = \beta_0 + \beta_1 x_1 + \beta_2 x_2$) to infer the genotypes of HB3 and 7G8: HB3 is 1 if β_2 is significant with p-values below 0.001; 0 otherwise; similarly for 7G8.

3.1 Accuracy

3.1.1 Proportions and number of strains
To validate our method we applied DEploid to 27 lab-mixed *in vitro* samples. As described in section 2.3.1, we start by assuming at most

sample	3D7	Dd2	HB3	7G8
PG0389-C	88.5 (90)	11.5 (10)	0	0
PG0390-C	79.8 (80)	20.2 (20)	0	0
PG0391-C	66.1 (67)	33.9 (33)	0	0
PG0392-C	31.2 (33)	68.8 (67	0	0
PG0393-C	18.4 (20)	81.6 (80)	0	0
PG0394-C	9.1 (10)	90.1 (90)	0	0
PG0395-C	0	33.6 (33.3)	35 (33.3)	31.3 (33.3)
PG0396-C	0	25.9 (25)	26.1 (25)	48 (50)
PG0397-C	0	14.7 (14.3)	15.3 (14.3)	69.9 (71.4)
PG0398-C	0	0	45.1+54.9 (100)	0
PG0399-C	0	0	56.7+40.9 (99)	2.4 (1)
PG0400-C	0	0	39.5+57.5 (95)	3 (5)
PG0401-C	0	0	33.3+56.7 (90)	10 (10)
PG0402-C	0	0	85.2 (85)	14.8 (15)
PG0403-C	0	0	80.1 (80)	19.3 (20)
PG0404-C	0	0	75.4 (75)	24.6 (25)
PG0405-C	0	0	70.6 (70)	29.4 (30)
PG0406-C	0	0	61 (60)	39 (40)
PG0407-C	0	0	50.5 (50)	49.5 (50)
PG0408-C	0	0	40.1 (40)	59.2 (60)
PG0409-C	0	0	30.1 (30)	69.1 (70)
PG0410-C	0	0	25.9 (25)	73,4 (75)
PG0411-C	0	0	21.4 (20)	78.5 (80)
PG0412-C	0	0	15.2 (15)	84.8 (85)
PG0413-C	0	0	3.8 (5)	96.2 (95)
PG0414-C	0	0	0 (1)	29.9+70.1 (99)
PG0415-C	0	0	0	30.0+70.0 (100)

Table 2. Experimental validation of the DEploid method. Inferred percentages (true values in brackets) of the mixed samples. In some cases DEploid identifies two near identical strains due to some erroneously called heterzyous sites. The "+" sign indicates the combined proportion.

three strains present in the mixtures; and discard strains with an inferred proportion less than 1%. DEploid successfully recovers the proportions with haplotypes of the input (see Table 2). The deviation between our proportion estimates and the truth is at most 2%.

In some cases, DEploid overfits lab-mixed samples with additional strains. For example, in Table 2, we infer six of the HB3 and 7G8 mixtures as mixing of three, two of which are near identical, but seperated because of a few heterozygous sites with high coverage resulting in high leverage in our model (Supplemental Material Figure S3.3(a)). These sites are likely artefacts arising from duplicated sequence that is absent from the reference strain. Such erroneous markers are not currently inferred by DEploid, though this could be included in future versions.

To investigate how the accuracy of haplotype inference is affected by the quality of the reference panel (in terms of having haplotypes close to those present in the samples) we experimented with deconvoluting the 27 lab-mixed samples with the following reference panels:

- panel I: five Asian and five African clonal strains from the Pf3k(Pf3k, 2016) resource: PD0498-C, PD0500-C, PD0660-C, PH0047-Cx, PH0064-C, PT0002-CW, PT0007-CW, PT0008-CW, PT0014-CW, PT0018-CW.
- panel II: panel I with the addition of HB3;
- panel III: panel II with the addition of 7G8;
- panel IV: panel III with the addition of Dd2;

In all cases we estimated the number and proportion of strains accurately, for example Figure 2 y-axes show the proportions of strains Dd2/7G8/HB3 as approximately $\frac{1}{4}/\frac{1}{2}/\frac{1}{4}$.
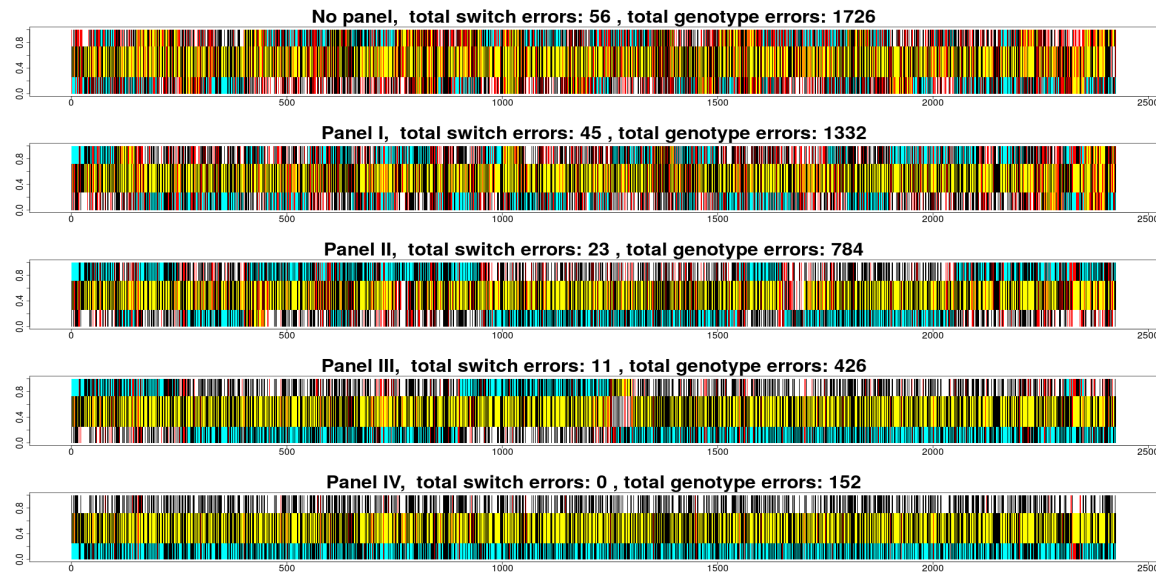
Fig. 2. Comparison of true and inferred haplotypes for Chromosome 14 in sample PG0396-C without any reference strain (top) and with using reference panels I to IV (from the second to the bottom). Black bars indicate alternative alleles; red bars mark wrongly inferred positions. The yellow, cyan and white background label the haplotype segments from strains 7G8, HB3 and Dd2 respectively. The switch errors are obtained by counting the changes of a strain segment mapped to reference strains; the genotype errors are the discordance between the strain and the mapped reference segments.

3.1.2 Haplotypes

Our accuracy assessment for inferred haplotypes takes into account both switch errors and genotype discordance, which reflects recombination and misscopying events. To understand how the inferred haplotypes relates to those present we split haplotypes into sets of 50 consecutive variants and assigned them to the reference strains through maximal identity. Switches occur when adjacent segments of inferred haplotypes are closest to different reference strains. Genotyping errors occur when a subset of sites within the segment differ from the closest reference strain. Example deconvolutions are shown in Figure 2 and an overview of all experiments is shown in Figure 3. From our assessment of haplotype inference, we conclude:

- The inference of relative proportions does not seem to be affected by the use of a reference panel or its quality (Figure 2).
- The accuracy of the haplotype is dependent on having an appropriate reference panel (Figure 2).
- The strain proportion affects the haplotype inference (see Fig 3). Our method infers strains with proportions over approximately 20% with high accuracy accuracy, but struggles with minor strains due to insufficient data, in particularly at sites when the minor strain carries the alternative allele and the dominant strain carries the reference allele (see Figure 3).

3.2 Run-time

The complexity of our program is $\mathcal{O}(lm^2)$ (see Fig 4), where m and l are the number of reference strains and sites respectively. In practice, we recommend dividing samples into distinct geographical regions to perform deconvolution, using the ten most different local clonal strains as as reference panel. The run time of deconvoluting a field sample range between 1 and 6 hours, depending on the number variants in a sample: For example, it takes $5\frac{1}{2}$ hours to process sample QG0182-C over 372,884 sites.
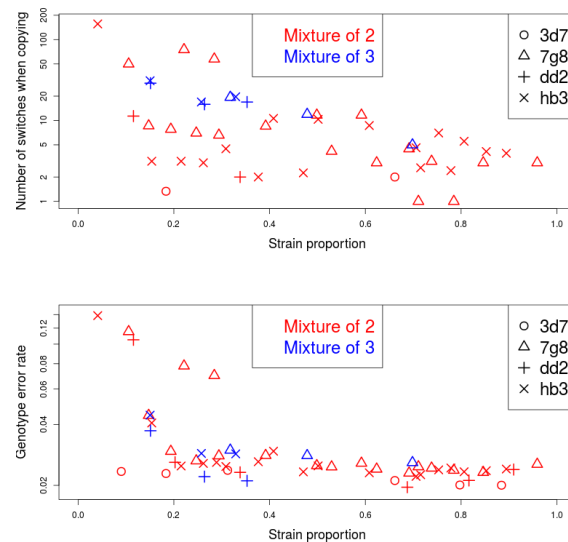

Fig. 3. Relationship between strain proportion and inference accuracy in the experimental validation. We use reference panel V to deconvolute all 27 samples. Each point represents a deconvoluted haplotype with 18,570 sites. Point shape refers to strain and colour indicates whether it was in mixture with two (red) or three (blue) strains. Top panel shows switch error rate. Bottom panel indicates genotyping error rate.

4 Discussion

The program `DEploid` and its analysis pipeline has been originally developed for *P. falciparum* studies. Nonetheless, with minor parameter changes, `DEploid` can be used for deconvoluting any other data set with a mixture of samples from a single species, for example on data from *Plasmodium vivax* (Pearson et al., 2016) or bacterial and viral pathogens.
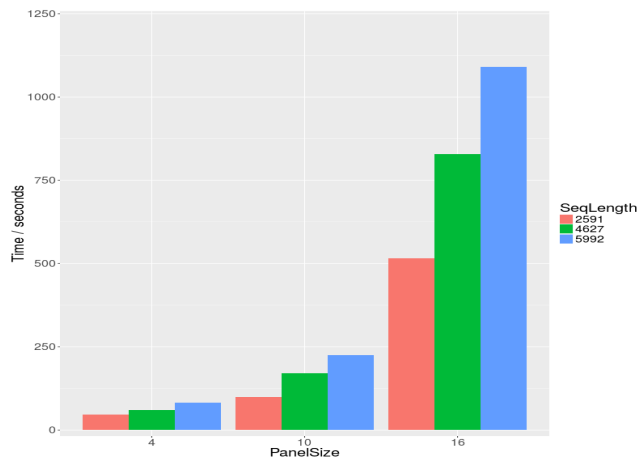
Fig. 4. Run-time and scaling. CPU time (seconds) for deconvoluting chromosomes 12, 13 and 14 of sample PG0412-C with reference panels I, V and VI, where panel V contains 3D7, HB3, 7G8 and Dd2 strains; and panel VI is equivalent to panel I with the addition of six clonal strains from Asia and Africa: PH0193-C, PH0283-C, PH0305, PT0060-C, PT0146-C and PT0158-C. The run-time is approxmately linear with respect to the number of sites and shows the expected quadratic trend against the number of reference strains.

There are several limitation of the current implementation, the greatest of which is the quadratic scaling with reference panel size. In practice, current approaches to related problems such as haplotype phasing (Delaneau et al., 2012) or inference from low-coverage sequencing experiments (Davis, 2016) typically aim to select a few candidate haplotypes (which might be a mosaic) from a reference panel. Alternatively, the reference panel data can itself be approximated, for example through graphical structures, as in BEAGLE (Browning and Browning, 2007), or represented through structures that enable efficient computation (Lunter, 2016). Such extensions will be pursued in future work. Similarly, the observation that a small number of erroneous heterozygous sites can lead to inferring the presence of closely related strains should be addressed. In some cases such sites may reflect *in vivo* evolution, but ideally these should be identified automatically and excluded.

Acknowledgements

Funding

References

Anita, D. (1998). Unstable malaria in Sudan: the influence of the dry season: clone multiplicity of *Plasmodium falciparum* infections in individuals exposed to variable levels of disease transmission. *Transactions of The Royal Society of Tropical Medicine and Hygiene 92*(6), 580–585.

Bell A. S. *et al.* (2006) Within-host competition in genetically diverse malaria infection: parasite virulence and competitive success. *Evolution 60*(7), 1358–1371.

Browning, S. R. and B. L. Browning (2007) Rapid and accurate haplotype phasing and missing-data inference for whole-genome association studies by use of localised haplotype clustering. *The American Journal of Human Genetics 81*(5), 1084–1097.

Davies, R. W. *et al.* (2016) Rapid genotype imputation from sequence without reference panels *Nature Genetics 48*, 965–969. doi:10.1038/ng.3594.

Delaneau, O. *et al.* (2012) A linear complexity phasing method for thousands of genomes. *Nat Methods 9*(2), 179–181.

de Roode, J. *et al.* (2004) Competitive release of drug resistance following drug treatment of mixed *Plasmodium Chabaudi* infections. *Malaria Journal 3*(33), 1–6.

de Roode, J. *et al.* (2005) Virulence and competitive ability in genetically diverse malaria infections. *Proceedings of the National Academy of Sciences of the United States of America 102*(21), 7624–7628.

Galinsky, K. *et al.* (2015) COIL: a methodology for evaluating malarial complexity of infection using likelihood from single nucleotide polymorphism data. *Malaria Journal 14*(4), 1–9.

Harris K. and Nielsen R. (2013). Inferring Demographic History from a Spectrum of Shared Haplotype Lengths. *PLoS Genet 9/*(6). doi: 10.1371/journal.pgen.1003521

Hastings, I. and U. D'Alessandro (2000). Modelling a predictable disaster: the rise and spread of drug-resistant malaria. *Parasitology Today 16*(8), 340–347.

Howie, B. N. *et al.* (2009) A flexible and accurate genotype imputation method for the next generation of genome-wide association studies. *PLoS Genet 5*(6), 1–15.

Lawson D. J. *et al.* (2012) Inference of Population Structure using Dense Haplotype Data. *PLoS Genet 8*(1). doi: 10.1371/journal.pgen.1002453

Li, N. and M. Stephens (2003) Modeling linkage disequilibrium and identifying recombination hotspots using single-nucleotide polymorphism data. *Genetics 165*(4), 2213–2233.

Lunter, G. (2016) Fast haplotype matching in very large cohorts using the Li and Stephens model. *bioRxiv*, doi:10.1101/048280

MalariaGEN (2008) A global network for investigating the genomic epidemiology of malaria. *Nature 456*(7223), 732 – 737.

Manske, M. *et al.* (2012) Analysis of plasmodium falciparum diversity in natural infections by deep sequencing. *Nature 487*(7407), 375–379.

Mathieson I. and McVean G. (2014). Demography and the Age of Rare Variants. *PLoS Genet 10*(8), doi: 10.1371/journal.pgen.1004528

Miles, A. *et al.* (2015) Indels, structural variation, and recombination drive genomic diversity in *Plasmodium falciparum*. *Genome Res 26*, 1288–1299.

Pearson, R. D. *et al.* (2016) Genomic analysis of local variation and recent evolution in Plasmodium vivax. *Nat Genet 48*, 959–964.

O'Connell J., *et al.* (2014) A General Approach for Haplotype Phasing across the Full Spectrum of Relatedness. *PLOS Genetics 10*(4), e1004234.

The Pf3k Project: pilot data release 5 (2016) www.malariagen.net/data/pf3k-5 [accessed 1 June 2016]

O'Brien D,J. *et al.* (2016) Inferring Strain Mixture within Clinical *Plasmodium falciparum* Isolates from Genomic Sequence Data. *PLoS Comput Biol 12*(6): e1004824. doi: 10.1371/journal.pcbi.1004824

Sabeti1. P. C. *et al.* (2002) Detecting recent positive selection in the human genome from haplotype structure. *Nature 419*, 832–837. doi:10.1038/nature01140

Wendler, J. (2015) *Accessing complex genomic variation in* Plasmodium falciparum *natural infection*. Ph. D. thesis, University of Oxford.

WHO. (2016) World Malaria Report 2015. *World Health Organization*.